Journal of
Nanoscience and Nanotechnology
Vol. 8, 1404–1409, 2008

Effects of High Pressure on the Luminescent Properties of Nanocrystalline and Bulk Y_2O_3:Eu^{3+}

X. Bai[1], H. W. Song[1,*], B. B. Liu[2], Y. Y. Hou[2], G. H. Pan[1], and X. G. Ren[1]

[1]*Key Laboratory of Excited State Physics, Changchun Institute of Optics, Fine Mechanics and Physics, Chinese Academy of Sciences, Changchun 130033, People's Republic of China and The Graduate School of Chinese Academy of Sciences, Changchun 130033, People's Republic of China*
[2]*National Laboratory of Superhard Materials, Jilin University, Changchun 130012, People's Republic of China*

High pressure-induced spectral changes in a 20-nm cubic nanocrystalline yttria doped with europium and its corresponding bulk were studied in the range of 550–750 nm, corresponding to the $^5D_0 \rightarrow {}^7F_J$ ($J = 0$–4) transitions. The results demonstrate that the bulk Y_2O_3 underwent phase transition from the cubic phase to the monoclinic phase as the pressure increased to 15 GPa, while the 20-nm nanocrystals did not. This can be concluded from the fact that the $^5D_0 \rightarrow {}^7F_0$ line and the three $^5D_0 \rightarrow {}^7F_1$ sublines originating from the cubic phase disappeared, while another group of $^5D_0 \rightarrow {}^7F_0$ and $^5D_0 \rightarrow {}^7F_1$ lines appeared. In addition, the relative intensity of the peak around 630 nm to that around 611 nm varied obviously as the pressure surpassed 15 GPa. The variations in the nanocrystals were more sluggish in comparison to those in the bulk, indicating that the nanocrystalline yttria had improved compressibility, which is attributed to an increased surface energy in nanocrystals. The local environment surrounding luminescent Eu^{3+} in the nanocrystals and the bulk both became more disordered with the increase of the pressure. The phase transition from the cubic to the monoclinic is irreversible.

Keywords: Y_2O_3:Eu^{3+}, High Pressure, Luminescent Properties.

RESEARCH ARTICLE

1. INTRODUCTION

In recent years, the high-pressure studies on nanocrystals (NCs) have stimulated great enthusiasm because the size of the NCs has a significant effect on the structural transitions and compressibility.[1–3] Understanding the mechanisms governing structural transitions not only offers opportunities for investigating the pressure dependence of electronic transport and optical and mechanical properties,[4] but also can help to bring about future developments in nanomaterials and devices.[5] Up to now, many studies have been performed on structural phase transitions in semiconductor NCs.[6–8]

For NCs doped with trivalent rare earth ions, Y_2O_3 in particular has attracted considerable interest due to its high chemical durability and thermal stability.[9,10] Eu^{3+}-doped yttria, as the main and unsurpassed red emitting material in fluorescent lamps and projection television tubes, is inevitably attracting increased attention.[11–13] Since the Eu^{3+} ion has very sharp emissions and its electronic dipole transitions of $^5D_0 \rightarrow {}^7F_2$ are supersensitive to the surrounding environments according to the J-O theory,[14,15] this ion was chosen as a luminescent probe of the crystalline environment.[16] In comparison with other luminescent materials involving strong electron-phonon coupling, the Eu^{3+}-doped materials can better reflect changes of the crystalline field structure of the host under pressure. However, the pressure effect on the luminescent properties of Y_2O_3:Eu^{3+} is unknown, and there have been no reports on this subject up to now. In this paper, we studied and compared the luminescent properties of Y_2O_3:Eu^{3+} NCs with corresponding bulk materials under high pressure up to 25 GPa. A few investigators have reported studies of the pressure-spectra of bulk yttria; however, in their work the pressure range is within several hundred Kbar, which is far less than in this work.[17]

2. EXPERIMENTAL DETAILS

The Y_2O_3:Eu^{3+} NCs were prepared by the combustion method. Y_2O_3 and Eu_2O_3 (molar ratio 1:0.01) were dissolved in nitric acid, and glycine was dissolved in distilled water. The two solutions were then mixed together to form the precursor. Details of the synthesis are given elsewhere.[18] The particle size was controlled by adjusting the molar ratio of glycine to metal nitrate (G/N),

*Author to whom correspondence should be addressed.

1533-4880/2008/8/1404/006 doi:10.1166/jnn.2008.351

which affected the combustion temperature in the reaction. In the preparation, the G/N ratio was controlled at 1.25. The bulk powders were prepared by the solid-state reaction method at 1,200 °C for 8 h. The pressure was generated by a diamond anvil cell technique using a stainless steel gasket. The gasket was preindented to 500 μm of thickness, and then a hole with a diameter of 100 μm was made in its center with a spark driller. The pressure medium was a methanol and ethanol mixture with a ratio of 4:1. The pressure in all the experiments was determined by a standard method: monitoring the shift of the ruby R1 line. Photoluminescence measurements under applied hydrostatic pressure were performed at room temperature. 514-nm light from a He-Cd laser was used as excitation source. The photoluminescence signals were collected with a JYHR800 spectrometer equipped with a charge coupled device (CCD) detector. Crystal structure and size were obtained by X-ray diffraction (XRD) using a Cu target radiation source.

3. RESULTS AND DISCUSSION

The crystal structure and particle size were obtained by XRD patterns, as shown in Figure 1. According to JCPDS standard cards, both the NCs and bulk exhibit pure cubic structure. The average crystalline size of the NCs was estimated by the Scherrer formula, to be ~20 nm.

Figure 2 shows the evolution of the emission spectra with pressure for NCs (a) and bulk (b). Under ambient conditions, the peak at 580.5 nm is from the $^5D_0 \rightarrow {}^7F_0$ transition, the lines at 587, 593 and 599.4 nm are from $^5D_0 \rightarrow {}^7F_1$ transitions, the lines in the range of 600–640 nm are from $^5D_0 \rightarrow {}^7F_2$ transitions, the lines in the 647–667 nm range are from the $^5D_0 \rightarrow {}^7F_3$ transitions, and the lines in the range of 680–720 nm are from the $^5D_0 \rightarrow {}^7F_4$ transitions. From Figure 2, it is obvious that the emission intensity of $^5D_0 \rightarrow {}^7F_J$ decreases, all transition lines show a shift toward longer wavelengths, and their half-widths increase with pressure during the process of loading pressure. The increased line width suggests that the local environment surrounding the Eu^{3+} ions becomes more disordered. During the process of unloading pressure, the emission intensity increases, and the spectral position shifts toward shorter wavelengths but does not recover completely at ambient pressure, indicating that the transformation is irreversible.

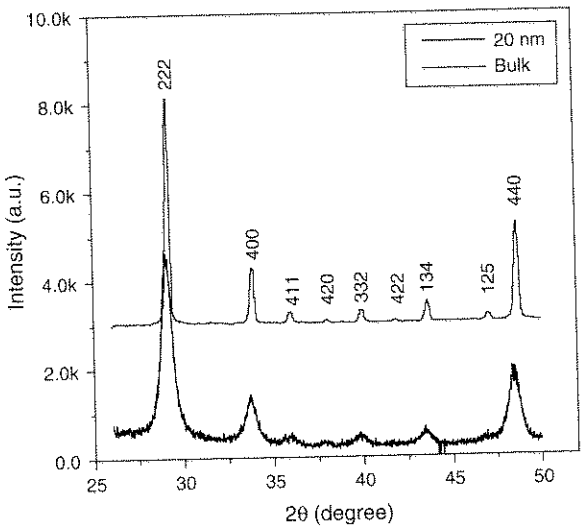

Fig. 1. XRD patterns of the Y_2O_3:Eu^{3+} NCs and bulk samples.

Figure 3 shows the normalized emission of $^5D_0 \rightarrow {}^7F_{0,1,2}$ for both samples. From Figures 3(a) and (b), under ambient conditions, we can see that the $^5D_0 \rightarrow {}^7F_0$ transition locates at 580.5 nm, and the $^5D_0 \rightarrow {}^7F_1$ transition splits into three peaks located at 587.3 nm, 593.1 nm and 599.4 nm. No distinct differences in line position were observed for the two samples, and no emission line assigned to the monoclinic phase was detected,[19, 20] which is consistent with the result of the XRD patterns. Note that in Figure 3 the peaks labeled with a star are associated with the $^5D_1 \rightarrow {}^7F_3$ transitions.[21] Under pressure, the separations among three peaks always changed less in both samples. In the bulk, it is interesting to observe that three additional peaks located at 597.4 nm, 592.5 nm, and 587.1 nm arise as the pressure increases to 15 GPa, indicating the occurrence of structure transition of the yttria host.[22] When the pressure reaches 17 GPa, the original three peaks are quenched completely. This result reveals that the pressure-induced structural transition is complete. However, in the NCs no additional peaks are found as the pressure increases. It is considered that in NCs the increased surface energy impedes the formation of the high-pressure phase and thus elevates the phase transition pressure owing to the existence of vast surface adsorptions such as OH^- and CO_3^{2-}.[17, 26]

For the $^5D_0 \rightarrow {}^7F_2$ transitions shown in Figures 3(c) and (d), it is clear that group A is triplet with a main peak at 611.4 nm and two shoulder peaks at 613.1 and 614.5 nm, while group B is doublet with a main peak at 631.4 and a shoulder at 627 nm, which all correspond to the transitions from the $^5D_0$ level to different $^7F_2$ sublevels $(2J+1)$. During the process of loading pressure, the intensity ratio of transitions from the $^5D_0$ level to different $^7F_2$ sublevels varies obviously with the pressure, and the total Stark components of the $^5D_0 \rightarrow {}^7F_2$ transitions increase with the increasing pressure.

Figures 4(a) and (b) show the emissions of $^5D_0 \rightarrow {}^7F_3$ and $^5D_0 \rightarrow {}^7F_4$, respectively. The peaks of the $^5D_0 \rightarrow {}^7F_3$ transitions are located at 650.7 nm, 653.4 nm, 658.2 nm, and 662.7 nm. The peaks of the $^5D_0 \rightarrow {}^7F_4$ transitions are located at 687.8 nm, 693.9 nm, 707.3 nm, 709.4 nm, and 712.6 nm. The peaks labeled with a star are the emission of the ruby. During the process of loading pressure, the intensity ratio of the transitions from the $^5D_0$ level to different $^7F_{3,4}$ sublevels and the Stark components of the $^5D_0 \rightarrow {}^7F_{3,4}$ transitions hardly change.

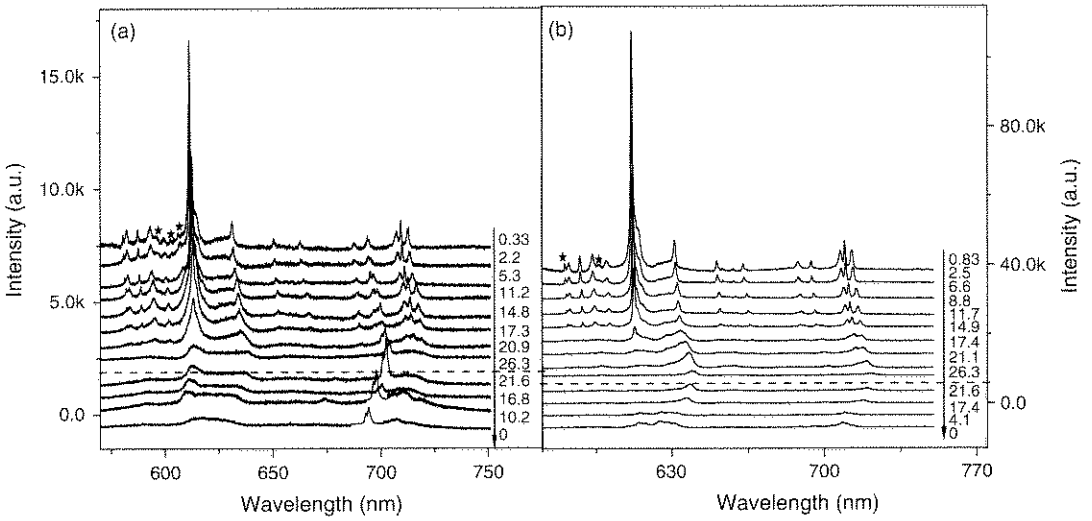

Fig. 2. Emission spectra for the both samples at various pressures under 514 nm excitation, (a) NCs; (b) bulk sample.

Figure 5 shows the peak positions of $^5D_0 \rightarrow {}^7F_1$, $^5D_0 \rightarrow {}^7F_2$, $^5D_0 \rightarrow {}^7F_3$, and $^5D_0 \rightarrow {}^7F_4$ as a function of applied pressure. The evolution of the peak positions of the $^5D_0 \rightarrow {}^7F_2$ transitions appeared to be almost uniform and linear until the applied pressure approached to 15 GPa. Above 15 GPa, the peak positions deviated from a linear relationship. The nonlinear relationship between the peak location and pressure for the $^5D_0 \rightarrow {}^7F_2$ transitions

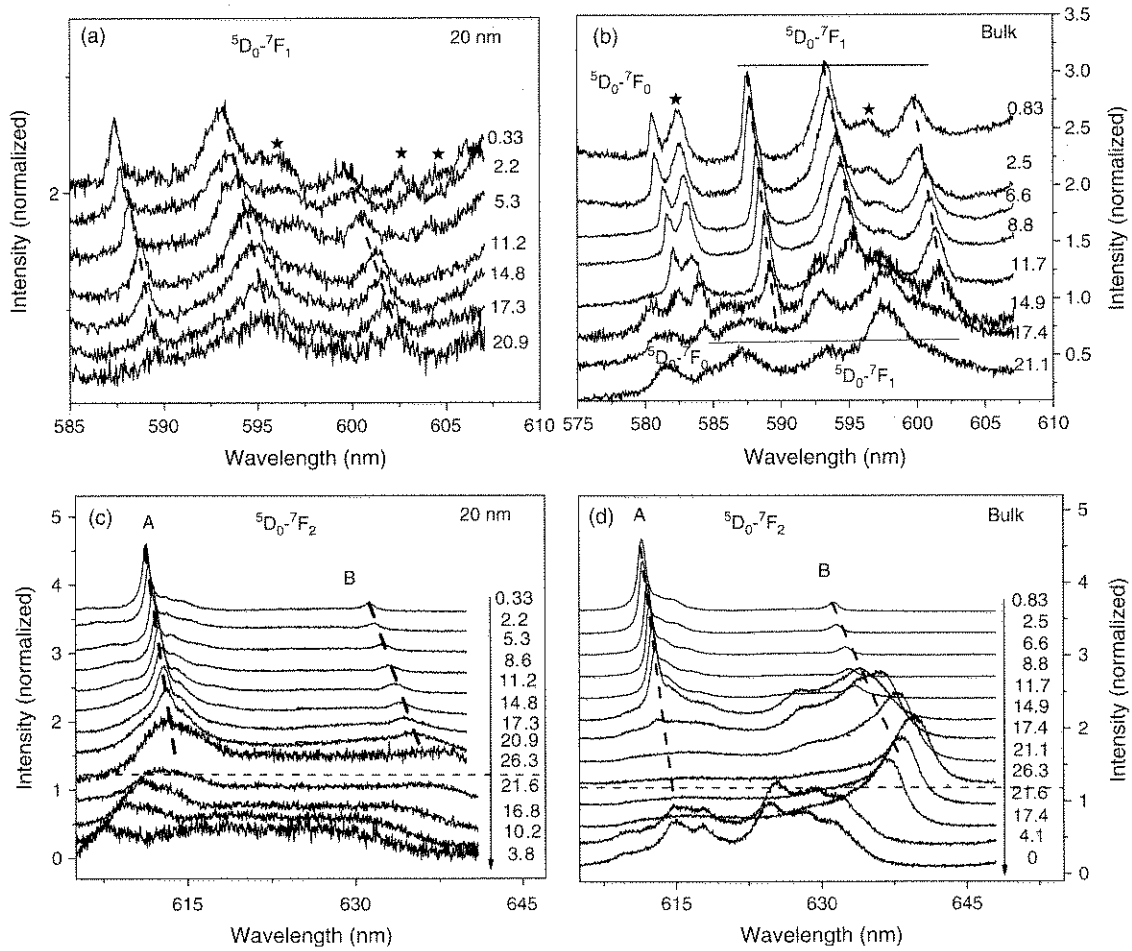

Fig. 3. The normalized emissions of $^5D_0 \rightarrow {}^7F_1$ and $^5D_0 \rightarrow {}^7F_2$ for both samples at various pressure under 514 nm.

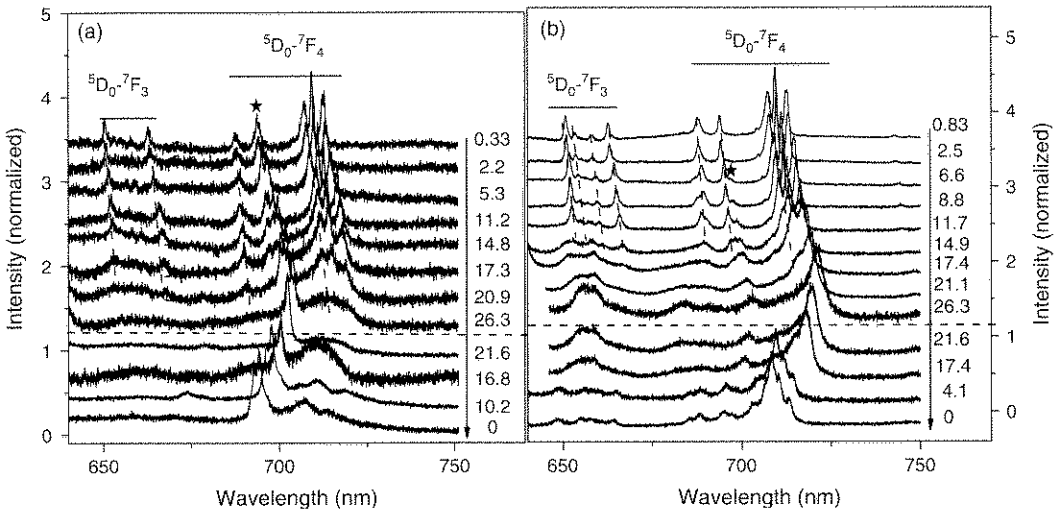

Fig. 4. The normalized emissions of $^5D_0 \rightarrow {}^7F_3$ and $^5D_0 \rightarrow {}^7F_4$ for both samples at various pressure under 514 nm, (a) NCs; (b) bulk samples.

is attributed to the structure transitions of the host. As the pressure increased, the line widths broadened, and the relative contributions for different sub-states varied due to lattice distortion; as a consequence, it is hard to clearly distinguish them. For the $^5D_0 \rightarrow {}^7F_J$ ($J = 1, 3, 4$) transitions, the peak positions depended linearly on pressure. The pressure coefficients of the peaks are listed in Table I.

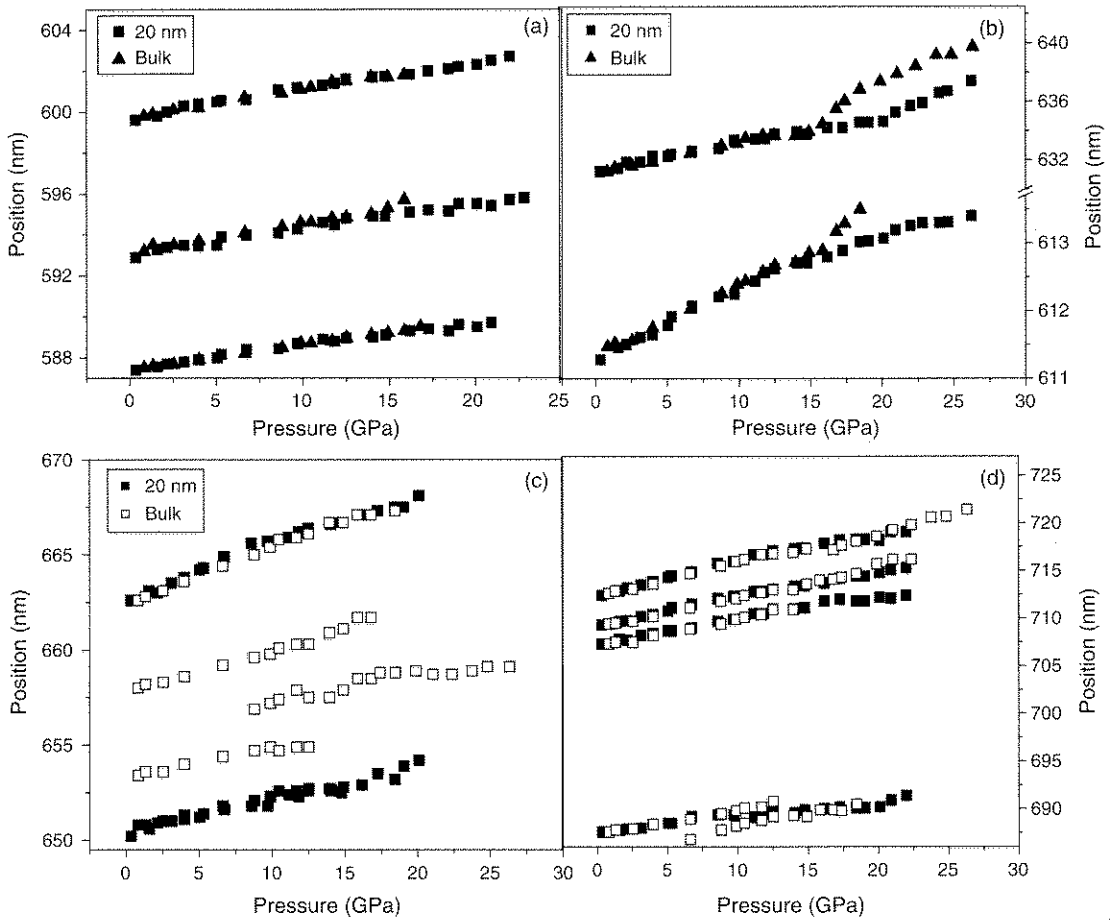

Fig. 5. Dependence of the peak positions on pressure for the Eu^{3+} ions emissions in Y_2O_3 samples, (a) the emissions originating from the energy level of $^5D_0 \rightarrow {}^7F_1$; (b) the emissions originating from the energy level of $^5D_0 \rightarrow {}^7F_2$; (c) the emissions originating from the energy level of $^5D_0 \rightarrow {}^7F_3$; (d) the emissions originating from the energy level of $^5D_0 \rightarrow {}^7F_4$.

Table I. Pressure coefficients of various emissions observed in the Y_2O_3:Eu^{3+} samples.

	$d\lambda/dP$ (nm/GPa)							
	587.3	593.1		599.4	611.4		631.4	
20 nm	0.107	0.12		0.131	0.102		0.184	0.34
bulk	0.123	0.144		0.138	0.101	0.23	0.198	0.48
	650.7	653.4	658.2	662.7	687.8	707.3	709.4	712.6
20 nm	0.17			0.27	0.14	0.24	0.27	0.31
bulk	0.16	0.13	0.12	0.23	0.25	0.29	0.32	0.33

Figure 6 shows the intensity ratios of groups A to B ($^5D_0 \rightarrow {}^7F_2$ transitions) at various pressures. Under applied pressure, The ratios increased at the same rate until the pressure reached 15 GPa, and then the rate increased faster in the bulk. Here we suggest that the samples were undergoing pressure-induced structure transition of the host as discussed above. This result is consistent with the previous studies that indicated the structure of yttria transforms from cubic to monoclinic when the pressure reaches 15 GPa.[22] The ratio of different transitions originating from the same $^5D_0 \rightarrow {}^7F_J$ levels varied obviously under loading pressure, indicating that the electron transition rates from the $^5D_0$ level to ^7F_J sublevels changed considerably with pressure.

We attribute these changes to the transformations of the crystalline field surrounding the Eu^{3+} ions resulting in the structural changes of the host. The pressure operated on the luminescence of Eu^{3+} ions in a crystalline environment mainly by modulating the symmetry and strength of the crystal field.[23] It is thought that the modulated crystal field results from the decreased cell parameter and equilibrium distance between the nucleus of the rare earth ions and the center of the ligand under high pressure.[24] The shift of line positions, increased half-width, and increased separations among Stark components with the pressure suggest the intensification of the crystal field under pressure.

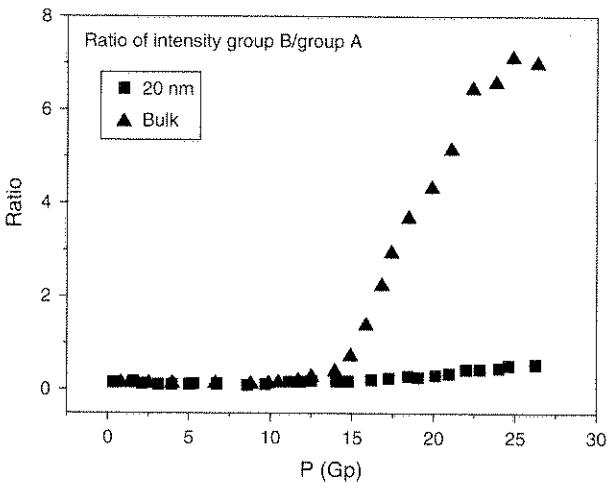

Fig. 6. The intensity ratio of group A to group B for the $^5D_0 \rightarrow {}^7F_2$ transition at various pressures.

By isomorphic substitution, Eu^{3+} occupy two symmetry sites in the Y_2O_3 host: a lower symmetry site of C_2 and a higher symmetry site of S_6. The observed transitions for Eu^{3+} essentially arise from those ions at C_2 site, where the degeneracy of all level of Eu^{3+} is completely lifted, splitting into $2J + 1$ sublevels.[21] The $^5D_0 \rightarrow {}^7F_2$ peaks are electronic dipole transitions, which are supersensitive to the surrounding environment according to the J-O theory,[14, 15] so the total splitting among the $^7F_2$ manifold increases more remarkably with increasing pressure than that of the $^7F_1$.

The results in Table I show that variations in NCs are more sluggish compared with the pressure-induced transformations in bulk, indicating that the compressibility increases as the particle size decreases. Because of the larger surface area-to-volume ratio, the local environment around Eu^{3+} ions in NCs is more complicated than that in the bulk. Considerable lattice distortion exists even in the absence of pressure,[25] so the changes of the local crystalline field in bulk materials may be more sensitive to pressure compared to the NCs. This sluggishness may due to the quasihydrostatic nature of the pressure. As the particle size decreases, the efficiency of transmitting the compressive stress from the pressure medium to the samples may improve, resulting in an enhancement of compressive stress.[1, 26]

4. CONCLUSIONS

The spectral properties of Y_2O_3:Eu^{3+} and the corresponding bulk material were studied and compared under loading and releasing pressure (0–25 GPa). The studies of the $^5D_0 \rightarrow {}^7F_0$ transitions demonstrate that in the bulk, the $^5D_0 \rightarrow {}^7F_0$ line and the three $^5D_0 \rightarrow {}^7F_1$ sublines originating from Eu^{3+} ions in the cubic phase gradually decreased with the increase of pressure. As the pressure increased to 15 GPa, another group of $^5D_0 \rightarrow {}^7F_0$ and $^5D_0 \rightarrow {}^7F_1$ emission lines appeared—which was attributed to the transitions of Eu^{3+} in the monoclinic phase—and the new peaks increased gradually with the increase of pressure. As the pressure reached 17 GPa, these three lines completely disappeared. This indicates that the transition from the cubic to the monoclinic phase began to occur at 15 GPa and completed at 17 GPa. In the nanocrystals, such a phase transition did not happen. The pressure-induced spectral changes for the $^5D_0 \rightarrow {}^7F_J$ transitions were irreversible. In addition, during the process of loading pressure, all the line positions for both samples revealed a shift toward longer wavelengths, the ratio of different transitions originating from the $^5D_0$ level varied obviously, and the energy separation between different $^7F_2$ sub-states increased. In the bulk, the ratio of $^5D_0$ to different sublevels of $^5D_2$ broke under the pressure of 15 GPa, which was also attributed to the structure transformation of the host. In conclusion, the nanocrystalline yttria demonstrated improved compressibility compared to the bulk, which was

attributed to the increased surface pressure caused by surface adsorption.

Acknowledgments: This work is supported by the National Nature Science Foundation of China (Grants 10704073, 50772042 and 10504030) and the 863 project of China (2007AA03Z314).

References and Notes

1. S. B. Qadri, J. Yang, B. R. Ratna, E. F. Skelton, and J. A. Hu, *Appl. Phys. Lett.* 69, 2205 (**1996**).
2. D. Srivastava, M. Menon, C. Daraio, S. Jin, B. Sadanadan, and A. M. Rao, *Phys. Rev. B* 69, 153414 (**2004**).
3. M. A. Makeev and A. Madhukar, *Phys. Rev. Lett.* 86, 5542 (**2001**).
4. B. B. Karki and R. M. Wentzcovitch, *Phys. Rev. B* 68, 224304 (**2003**).
5. H. Zhang, B. Gilbert, F. Huang, and J. F. Banfield, *Nature (London)* 424, 1025 (**2003**).
6. S. J. Chen, Y. C. Liu, C. L. Shao, C. S. Xu, Y. X. Liu, C. Y. Liu, B. P. Zhang, L. Wang, B. B. Liu, and G. T. Zou, *Appl. Phys. Lett.* 88, 133127 (**2006**).
7. N. J. Lee, R. K. Kalia, A. Nakano, and P. Vashishta, *Appl. Phys. Lett.* 89, 093101 (**2006**).
8. L. H. Shen, X. F. Li, Y. M. Ma, K. F. Yang, W. W. Lei, Q. L. Cui, and G. T. Zou, *Appl. Phys. Lett.* 89, 141903 (**2006**).
9. D. Matsuura, *Appl. Phys. Lett.* 81, 4526 (**2002**).
10. S. Xiao, X. L. Yang, Z. W. Liu, and X. H. Yan, *J. Appl. Phys.* 96, 1360 (**2004**).
11. X. Bai, H. W. Song, L. X. Yu, L. M. Yang, Z. X. Liu, G. H. Pan, S. Z. Lu, X. G. Ren, Y. Q. Lei, and L. B. Fan, *J. Phys. Chem. B* 109, 15236 (**2005**).
12. H. Z. Wang, M. Uehara, H. Nakamura, M. Miyazaki, and H. Maeda, *Adv. Mater.* 17, 2506 (**2005**).
13. H. Wang, C. K. Lin, X. M. Liu, and J. Lin, *Appl. Phys. Lett.* 87, 181907 (**2005**).
14. B. R. Judd, *Phys. Rev.* 127, 750 (**1962**).
15. G. S. Ofelt, *J. Chem. Phys.* 37, 511 (**1962**).
16. L. X. Yu, H. W. Song, S. Z. Lu, Z. X. Liu, L. M. Yang, and X. G. Kong, *J. Phys. Chem. B* 108, 16697 (**2004**).
17. P. A. Tanner, *J. Nanosci. Nanotechnol.* 5, 1455 (**2005**).
18. H. W. Song, B. J. Chen, H. S. Peng, and J. S. Zhang, *Appl. Phys. Lett.* 81, 1776 (**2002**).
19. D. K. Williams, B. Bihari, B. M. Tissue, and J. M. M. Chale, *J. Phys. Chem. B* 102, 916 (**1998**).
20. B. Bihari, H. Eilers, and B. M. Tissue, *J. Lumin.* 75, 1 (**1997**).
21. N. C. Chang and J. B. Gruber, *J. Chem. Phys.* 41, 3227 (**1964**).
22. E. Husson, C. Proust, P. Gillet, and J. P. Itie, *Mater. Resear. Bullet.* 34, 2085 (**1999**).
23. G. Huber, K. Syassen, and W. B. Holzapfel, *Phys. Rev. B* 15, 5123 (**1977**).
24. K. B. Keating and H. G. Drickamer, *J. Chem. Phys.* 34, 143 (**1961**).
25. T. Igarashi, M. Ihara, T. Kusunoki, K. Ohno, T. Isobe, and M. Senna, *Appl. Phys. Lett.* 76, 1549 (**2000**).
26. S. T. Tolbert and A. P. Alivisatos, *Science* 265, 373 (**1994**).

Received: 28 December 2006. Accepted: 24 May 2007.

RESEARCH ARTICLE